Intermetallic Growth Studies on Sn-Ag-Cu Lead-Free Solder Joints

JOHN H.L. PANG,[1,2] LUHUA XU,[1] X.Q. SHI,[1] W. ZHOU,[1] and S.L. NGOH[1]

1.—School of Mechanical & Production Engineering, Nanyang Technological University, Singapore 639798. 2.—E-mail: mhlpang@ntu.edu.sg

Solid-state intermetallic compound (IMC) growth behavior plays an important role in solder joint reliability of electronic packaging assemblies. The morphology and growth of interfacial IMC compounds between 95.5Sn-3.8Ag-0.7Cu Pb-free solders and nickel/gold (Ni/Au) surface finish on BGA solder joint specimen is reported. Digital imaging techniques were employed in the measurement of the average IMC growth thickness. The IMC growth behavior subjected to isothermal aging exposure at 125°C, thermal cycling (TC), and thermal shock (TS) with upper soak temperatures of 125°C are compared. An equivalent isothermal aging time is proposed for comparison of IMC layer growth data. It was noted that IMC layer growth under thermal cycling and thermal shock aging gives an acceleration factor of 1.4 and 2.3 based on the equivalent isothermal aging time.

Key words: Aging, intermetallic compound (IMC), lead free, reliability, solder joint, thermal cycling, thermal shock

INTRODUCTION

Lead-free solders will replace tin-lead solders due to legislation to ban lead (Pb) usage in electronic products. The electronic industry is preparing for Pb-free solder reflow manufacturing of electronics assemblies.[1] In the European Union, the WEEE and RoHS legislations will take effect on July 1, 2006. In North America, the National Electronics Manufacturing Initiative (NEMI) organization[2] provides industry with guidelines on lead-free solders and soldering solutions. The NEMI recommends lead-free 95.5Sn-3.9Ag-0.6Cu solder for solder reflow process.

Characterization of lead-free solder material properties, manufacturing process implementation, and board-level solder joint reliability performance are urgently needed. Studies on solder joint reliability characterizations of tin-silver-copper lead-free solder have been reported.[3,4] Materials and mechanical characterization of bulk solder and solder joint properties are needed to better understand Pb-free solder and solder joint deformation and failure behavior.[5–8] Thermal aging effects on IMC growth behavior for Pb-based[9] and Pb-free[10] solders need further research attention to correlate different thermal cycling aging profiles and isothermal aging effects.

In this study, the morphology and growth of interfacial IMC compounds between 95.5Sn-3.8Ag-0.7Cu Pb-free solders and nickel/gold (Ni/Au) surface finish were studied on a BGA solder joint specimen. Digital imaging techniques were employed in the measurement of the average IMC growth thickness. The IMC growth behaviors subjected to isothermal aging exposure at 125°C, thermal cycling, and thermal shock with an upper soak temperature of 125°C are compared.

EXPERIMENTAL PROCEDURES

The solder joint specimen fabrication process by solder reflow, temperature cycling aging experiments, and microstructure characterization will be discussed in the following subsections.

Fabrication of Solder Joint Test Specimens

The solder joint specimen consists of a single BGA 95.5Sn-3.8Ag-0.7Cu solder ball, soldered between two FR4 substrate materials, as shown in Fig. 1. This test specimen was used earlier for 63Sn-37Pb solder joint studies.[6] The Ni/Au surface finish on the copper

(Received March 11, 2004; accepted May 30, 2004)

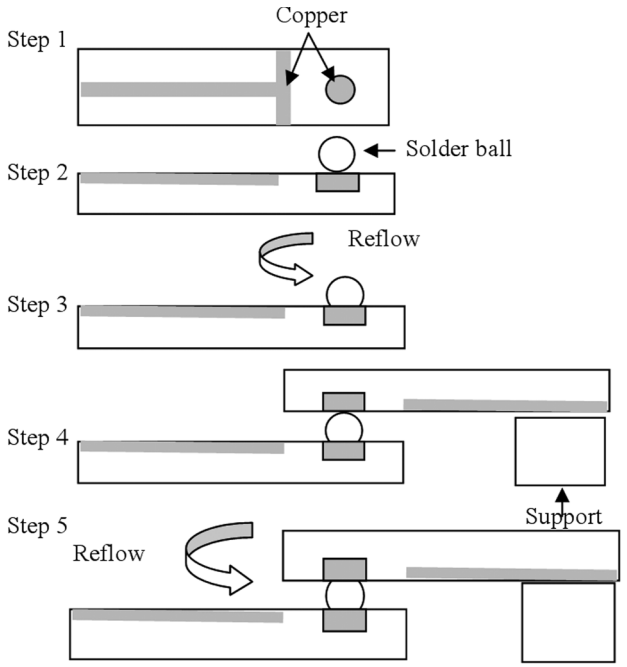

Fig. 1. Fabrication process for solder joint specimen.

pad has a nickel (Ni) layer thickness of 5 μm and a gold (Au) flash thickness of 0.3 μm. The copper pad thickness is 30 μm. The FR-4 substrate specimen pieces have dimensions of 12 mm × 3 mm × 0.5 mm. The specimen pieces are placed on a template for soldering. No-clean flux was applied onto the copper pad and a solder sphere is placed on top of the flux and reflowed on one side, as shown in Fig. 1. After the first reflow, another fluxed FR-4 piece is placed onto the template and the reflowed piece is flipped over a second FR-4 piece and reflowed for a second time to form a lap shear specimen. The solder reflow profile with a peak temperature of 250°C was used in the fabrication. For x-ray diffraction (XRD) experiments, some larger specimens (20 mm by 20 mm), with a 10-mm diameter solder (Sn-3.9Ag-0.6Cu) droplet, reflowed using the same profile were used for plan view XRD measurements of IMC structure after etching away the solder.

Isothermal Aging and Thermal Cycling Aging

Isothermal aging at 125°C, thermal cycling (TC), and thermal shock (TS) were used for solid-state IMC growth studies. Isothermal aging at 125°C was carried out in a thermal chamber for 47 h, 119 h, 167 h, and 262 h. The TC profile is –40°C to +125°C with a cycle time of 56 min, a ramp rate of 12.7°C/min, and hold time of 15 min. The TS profile is –55°C to +125°C with a cycle time of 17 min, a ramp rate of 51.4°C/min, and hold time of 5 min. The solder joints were subjected to TC and TS aging for 500 cycles, 1,000 cycles, and 2,000 cycles. The exposure time at 125°C is equal to the total dwell time spent at the high-temperature soak period for the TC and TS profiles, respectively. This is compared to the isothermal aging results at 125°C.

Characterizations

After thermal aging, the lap shear specimens were mounted, cross-sectioned, and polished for optical microscope investigation. Then they were etched (5% HNO_3 + 95% methanol) and observed with a JEOL JSM-5410LV (Japan Electron Optics Ltd., Tokyo) scanning electron microscope (SEM) under an accelerated voltage of 20 kV. Energy-dispersive x-ray analysis (EDX) was used to identify the material elements present in each selected area in the solder joint. Digital imaging techniques were employed in the measurement of the average IMC growth thickness (shown in Fig. 2). Two polylines, R1 and R2, were created manually along the edge of the IMC by using the tracing tool. Then, the average distance between the two polylines is given automatically. The thickness results were defined by spatial calibration. The minimum and maximum distances between the two lines are also marked in the image.

The phases formed at the interface were identified by the XRD analysis on the plan view by etching away the Sn matrix. The XRD analysis was conducted on a X-pert Powder Diffractometer employing Cu K_α radiation (λ = 1.5418 Å, DS = 0.25°). The x-ray tube was operated at 40 kV and 40 mA. The x-ray diffractograms were recorded at a step size of 0.02° in the range $10° \leq 2\theta \leq 120°$ with 5 sec count accumulation per step.

SOLDER JOINT MICROSTRUCTURE AND IMC GROWTH RESULTS

Characterization of As-Reflowed Solder Joint

The features of the microstructure and IMCs formed after reflow were observed with an SEM. The EDX was used to identify the material elements present in the solder joint. A low-magnification image of the entire solder joint is shown as Fig. 3, and the region of interest indicated by (I) and (II) will be discussed further. The microstructure of the solder joint after reflow typically consists of globular Sn-rich phases surrounded by small Ag_3Sn phases, and Cu_6Sn_5 is also present. Some large Ag_3Sn IMC rods are formed in the solder, and can be as long as 100 μm or more. The enlarged images of the regions

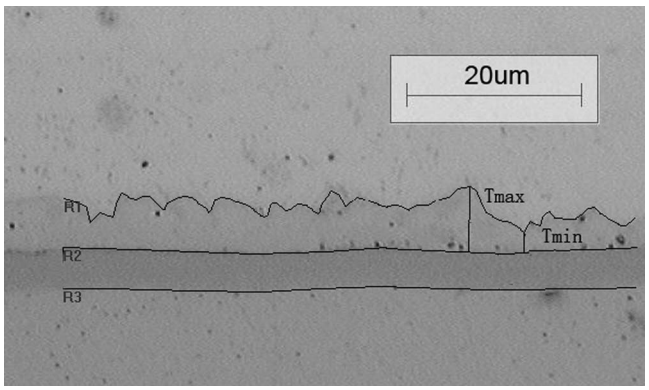

Fig. 2. Digital imaging techniques to measure the average IMC thickness.

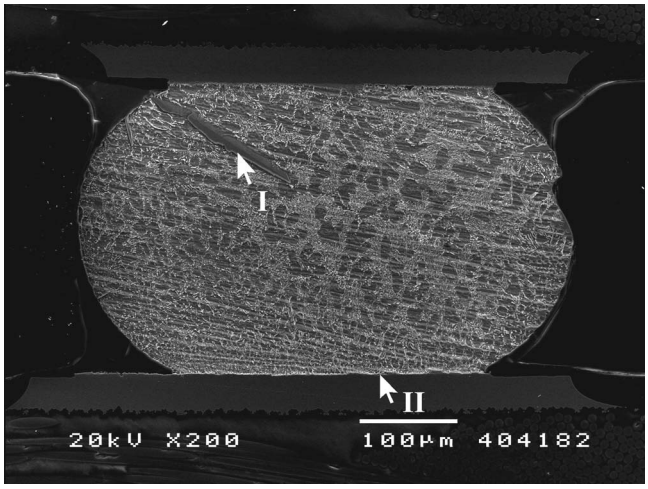

Fig. 3. Microstructure of solder joint after reflow.

(I) and (II) are shown in Figs. 4 and 5 together with the EDX spectrums.

Large Ag_3Sn rods can cause reliability concerns when they form in a high stress concentration area, such as the corner between solder bump and copper pad. Fatigue cracks can initiate and propagate along the interface between the Ag_3Sn and solder, leading to mechanical failure.[11] Sung et al.[12] reported that the growth of large Ag_3Sn is critically affected by the cooling rate during reflow. With a high cooling rate, such as 1.5°C/sec or higher, the formation of large Ag_3Sn can be suppressed. However, such a high cooling rate is not practical in real reflow operation. Thus, the solder reflow process generates nonuniform growth of eutectic structures. The SEM image in Fig. 4 shows the details of location (I) in Fig. 3, in which a large rodlike Ag_3Sn structure is present. Some smaller crystals of Cu_6Sn_5 were found near the Ag_3Sn rod. The Sn-rich phase forms first upon solidification, while the Ag and Cu in the remaining liquid phase reaches an extent for the IMC phases to nucleate a pseudoeutectic structure in the interdendritic spaces. Since Ag has a higher concentration compared to Cu, Ag_3Sn can nucleate and grow rapidly to a higher volume, such as the large one shown in Fig. 4 (I). The formation of Cu_6Sn_5 is found on the boundary of Sn-rich dendrites and Ag_3Sn regions. The EDX spectrum is also used to identify the presence of Ag_3Sn and Cu_6Sn_5, and this is compared with the reported EDX spectrums.[10] The actual composition of the IMC compound may be derived from phase diagrams and XRD studies.

The SEM image in Fig. 5 shows the morphology of solder/nickel interface, which is the enlarged image of location (II) in Fig. 3. EDX analysis was used to identify the traces of respective elements noted at the IMC layer. The darker phase above the IMC is

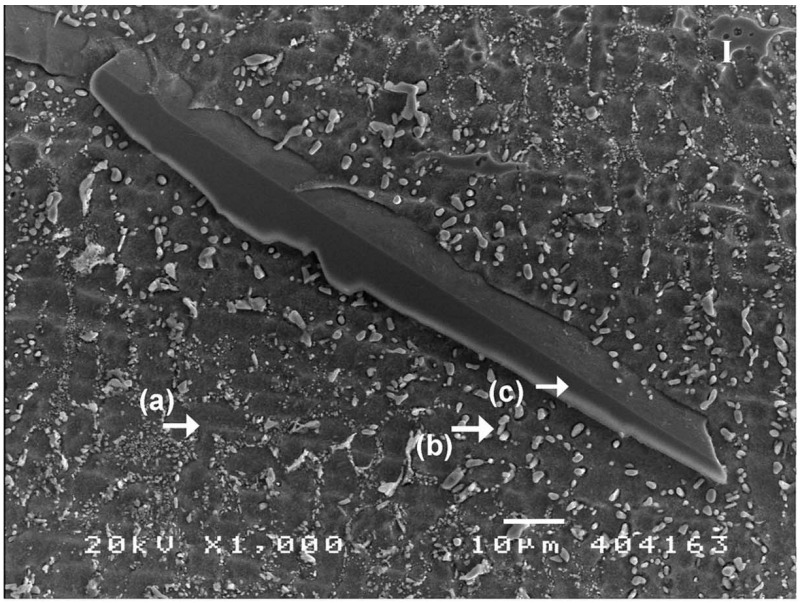

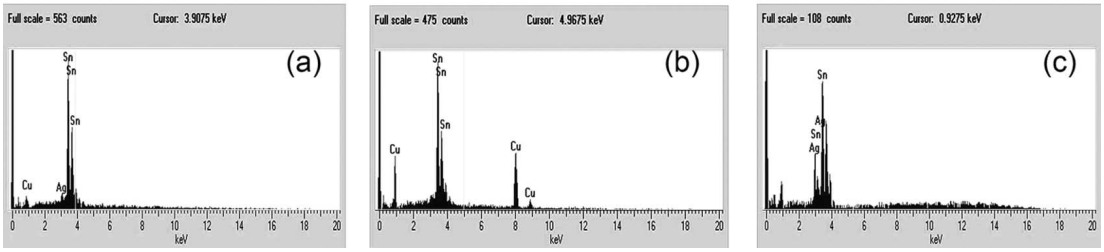

Fig. 4. IMC and EDX features in the solder joint (plot I in Fig. 3): (a) Sn-rich, (b) Cu_6Sn_5, and (c) Ag_3Sn.

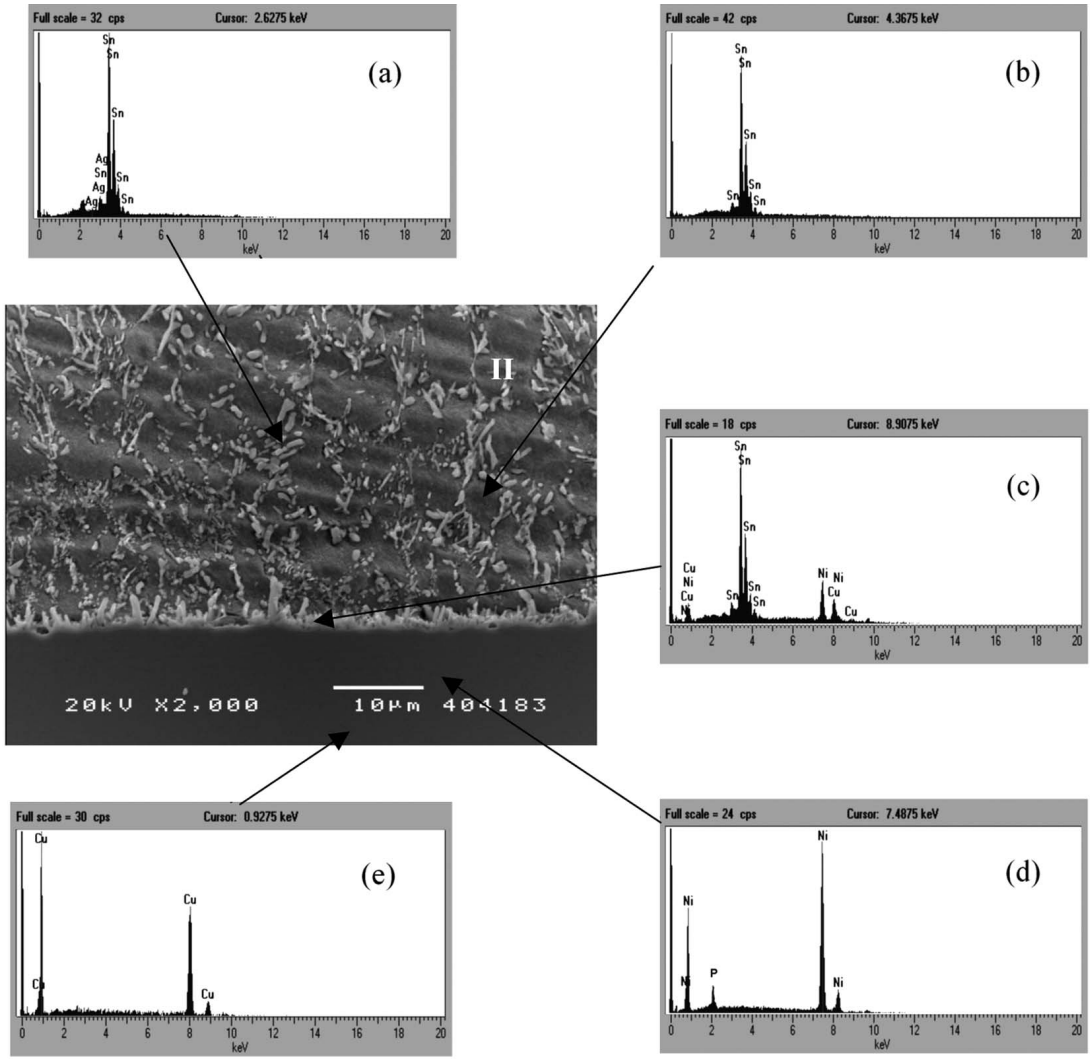

Fig. 5. IMC and EDX features at the solder/nickel interface (plot II in Fig. 3): (a) Ag_3Sn IMC, (b) Sn-rich, (c) Cu-Ni-Sn IMC, (d) Ni metallization layer, and (e) Cu pad.

the Sn-rich matrix, whereas the lighter features are Ag_3Sn and some Cu_6Sn_5 precipitates. The Ni metallization layer is approximately 5-μm thick, and contains about 6wt.%P. The darker phase below the Ni layer is the copper pad. The IMC formed between the solder and the Ni/Au surface finish on the copper pad is quite complex, as reported by Shiau et al.[10] Based on the EDX analysis in Fig. 5(c), it is possible to identify the exact phase and chemical composition. The elements Sn, Ni, and Cu were identified, but the thickness of the IMC after reflow is around 1 μm, which is very close to the minimal EDX spot size. To determine the composition and morphology of IMC at the solder/nickel interface, XRD measurements on a larger specimen prepared the same way were made. The IMC layer from the plan view is exposed after etching away the Sn matrix using 13 vol.% nitric acid in DI water. Both XRD and SEM were employed for phases and morphology studies on the layer. The XRD specimen has a 20 mm by 20 mm copper pad with the same Ni/Au plating and solder reflow procedure to form a 10-mm-diameter solder droplet. The plan view of the IMC is shown in Fig. 6. There are many needles like IMC located on the plan view, their typical size ranging from 5 μm to 10 μm in length and 1 μm to 2 μm in width. Figure 7 shows the XRD pattern of the plan view. The major phase turned out to be Ni_3Sn_4 by matching the search with the data from the International Centre for Diffraction Data, and peaks of Ni substrate can also be seen, but the intensity is much lower compared to Ni_3Sn_4. Combined with the EDX result that Cu is present in the needlelike IMC, it is actually Cu-substituted $(Ni_{1-x}Cu_x)_3Sn_4$. Based on Chen's study of the Sn-Cu-Ni ternary system and a Sn-Cu-Ni ternary phase diagram,[13] it can be seen that x, the portion of Cu here, can range from 0 to 0.10 while keeping the Ni_3Sn_4 crystal structure unchanged.

Interface IMC Growth Behavior Subject to Thermal Aging Exposure

Solder joints experience thermal cycling exposure due to cyclic environment thermal excursions and electronic equipment power on-off cycles. Therefore

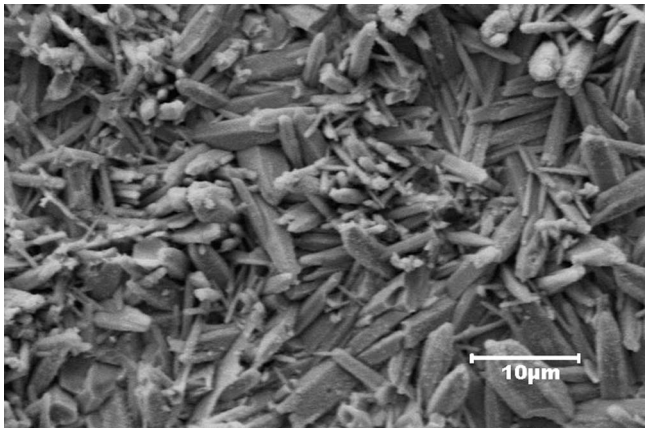

Fig. 6. Plan view of solder/nickel interface after etching away Sn matrix.

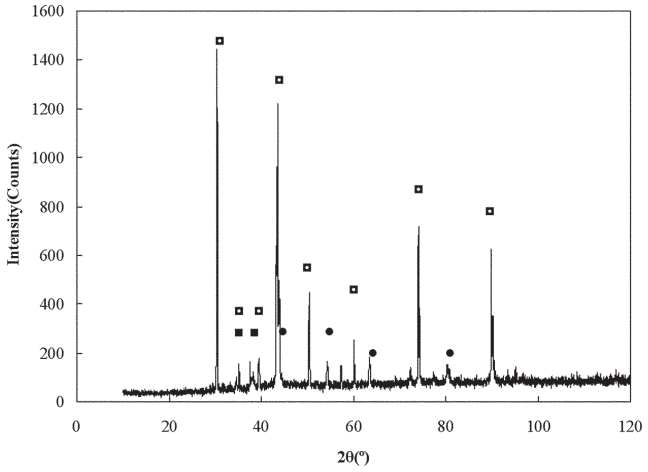

Fig. 7. XRD pattern of solder/nickel interface (plan view): (◘) Ni3Sn4, (■)Sn, and (•)Ni.

it is important to understand the effects of thermal cycling aging on the microstructure and IMC growth of solder joints subject to controlled thermal cycling exposure. A comparison of the morphology and the average IMC thickness on the interface were performed between isothermal, TC, and TS aging.

After isothermal aging for 47 h, 119 h, 167 h, and 262 h, the interface morphology were captured by optical microscopy and shown in Fig. 8. The measurements of the Cu-Ni-Sn IMC thickness were processed from the optical microscope images rather than the SEM images. By using the optical microscope, the needlelike $(Ni_{1-x}Cu_x)_3Sn_4$ IMC on the solder/nickel can be readily observed on a cross-sectional surface without etching. However, for SEM, the etching process must be used first before observing the IMC details. A problem is that those IMCs behind the surface can also be seen, as shown in Fig. 9. When using the digital imaging technique with such SEM images, a higher average IMC layer thickness will be computed. Thus, optical images were more suitable for determining the IMC layer thickness in this study.

Figure 9 shows the IMC morphology after 0 h, 119 h, and 262 h of isothermal aging at 125°C. It can be seen that after reflow (i.e., at 0 h), the IMCs on the solder/nickel interface are irregular and grow in a needlelike manner. After 119 h of aging, coalescence of the IMC needles leads to lateral thickening and ripening. After 262 h of aging, the IMC layer growth is planar in nature. For the TC and TS aging after 500 cycles, 1,000 cycles, and 2,000 cycles, the IMC morphologies are shown in Figs. 10 and 11, respectively. The IMC growth phases are similar to the isothermal aging case, beginning in a needlelike manner and finally turning into planar growth. After 500 cycles of TC or TS aging, the needlelike $(Ni_{1-x}Cu_x)_3Sn_4$ IMCs are almost immerged into the developed planner IMCs in solid state, and disappear after further aging.

METHOD FOR COMPARING IMC GROWTH FOR ISOTHERMAL AND TC AGING

Normally, TC and TS aging can lead to device failure in a shorter time; thus, they are often used as accelerated tests for reliability design. Since the thickness of the interfacial IMC is an important factor and can affect the device reliability, it is necessary to identify whether TC and TS have an effect on the IMC growth behavior. In this section, the IMC growth rates for isothermal, TC, and TS aging were compared by the following methods.

In order to simplify the comparison, the IMC growth was assumed to be volume diffusion controlled, i.e., the growth rate is proportional to the square root of time. The IMC thickness, x_t, subject to the aging time can be described by Eq. 1:

$$x_t = D\sqrt{t} + x_0 \tag{1}$$

where D is the diffusion coefficient; x_0 is the initial IMC thickness, and t, for isothermal aging, is the total aging time. The diffusion coefficient is given by an Arrhenius expression:

$$D = D_0 \exp(-Q/RT) \tag{2}$$

where D_0 is the diffusion constant, Q is the activation energy, R is universal gas constant, and T is the absolute temperature.

Since the temperature changes with time for TC and TS aging, the major issue for comparison is to determine the "effective aging time," t_{eff}, in terms of the time that mainly contributes to the IMC growth. From Eqs. 1 and 2, it can be seen that the diffusion coefficient D is the key factor in determining the growth rate, and D is a function of activation energy, Q, and temperature, T. The value of Q is 51.3kJ/mol, calculated from our work on isothermal aging at different temperatures. Using the TS aging as an example, and considering one cycle in the TS aging:

At 125°C, 5 min,

$$D_{125} = D_0 \exp(-5.13\times10^4/8.31\times398) = 1.84\times10^{-7}D_0$$

At −55°C, 5 min,

$$D_{-55} = D_0 \exp(-5.13\times10^4/8.31\times218) = 5.03\times10^{-13}D_0 = 2.74\times10^{-6}D_{125}$$

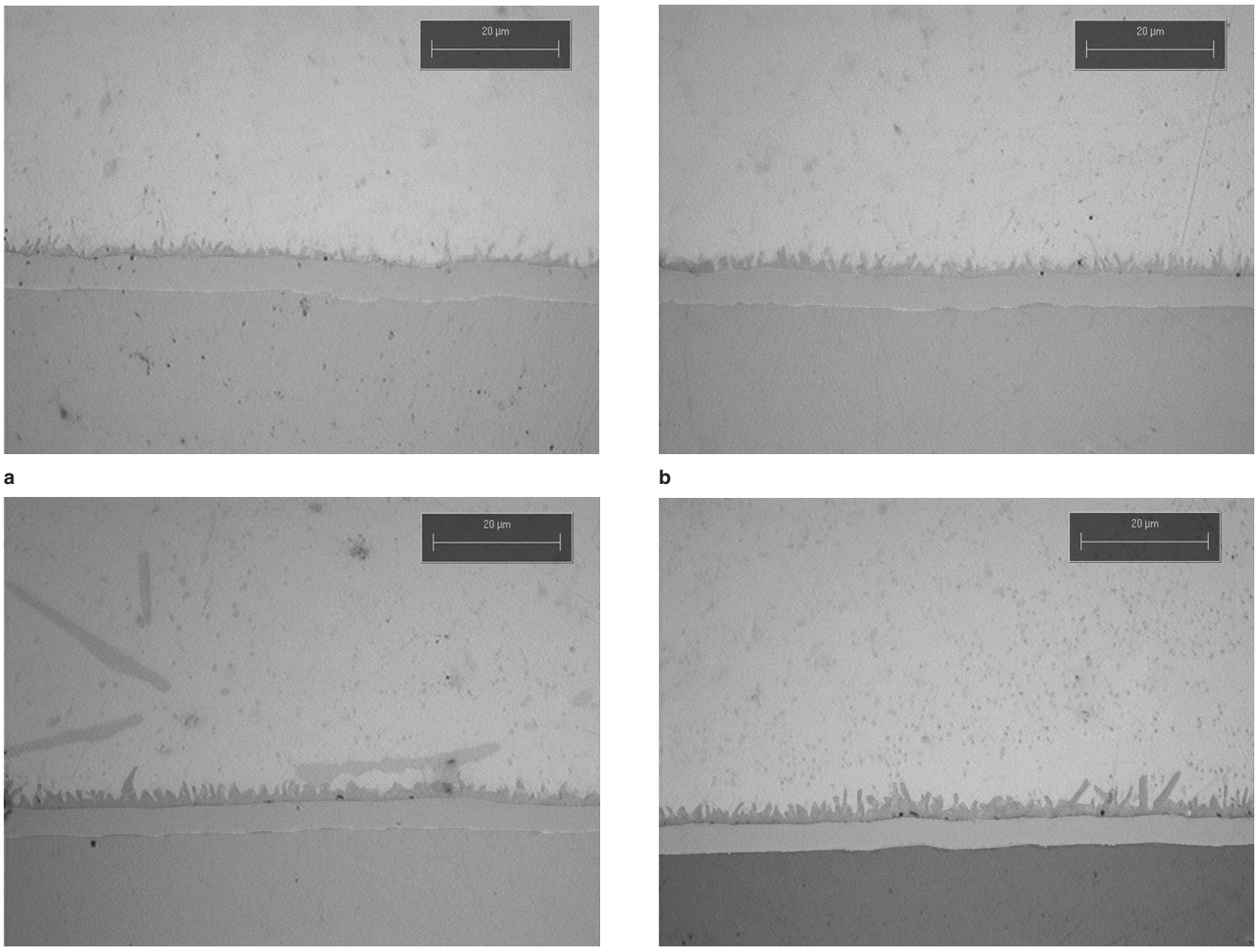

a b c d

Fig. 8. IMC thickness growth for isothermal aging (optical image): (a) 47 h, (b) 119 h, (c)167 h, and (d)262 h.

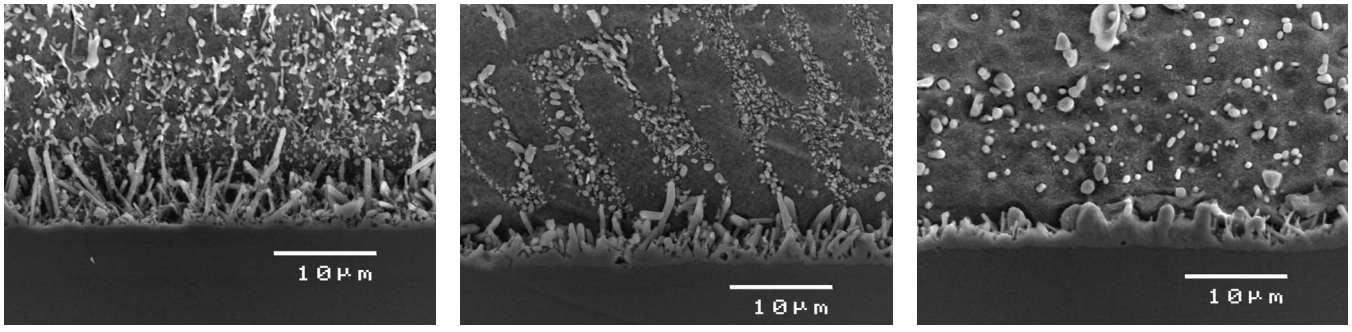

a b c

Fig. 9. IMC morphology change for isothermal aging (SEM image): (a) 0 h, (b) 119 h, and (c) 262 h.

At the ramp from −55°C to 125°C and reverse, 3.5 min each:

$$D_{ramp} = D_0 \exp(-5.13\times10^4/8.31T)$$

The diffusion coefficient D/D_{125} subject to time in one cycle is plotted in Fig. 12. It can be seen that during the ramp period, D_{ramp} drops to a very low value very quickly. In the lower soak temperature −55°C, the value of D_{-55} is only $2.74*10^{-6}$ times D_{125}. Hence, diffusion at a temperature lower than 125°C can be neglected for simplicity. It is reasonable to assume that only the upper soak temperature segments at 125°C of the cycles contribute mainly to IMC layer growth. The IMC growth at other segments of the TC and TS profile below 125°C is neglected. The effective aging time, t_{eff}, for both TC and TS, is defined as the total accumulated dwell time at 125°C. For TS aging between –55°C and

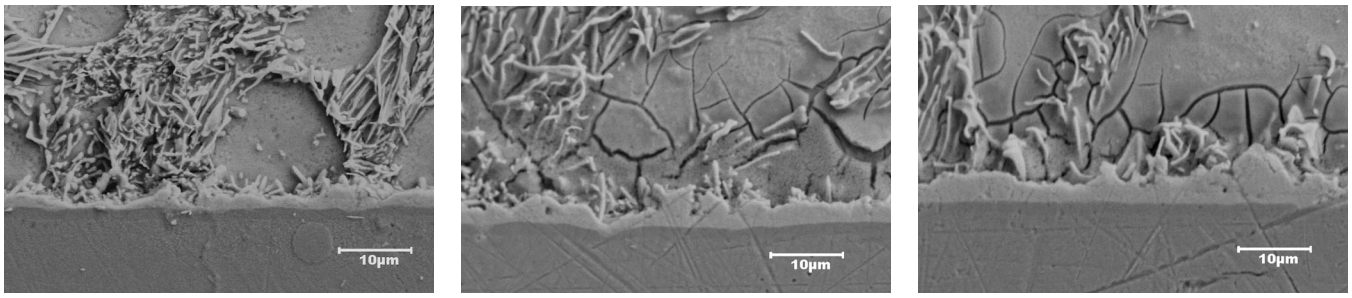

a b c

Fig. 10. IMC morphology change subject to thermal cycling (SEM image): (a) 500 cycles, (b) 1,000 cycles, and (c) 2,000 cycles.

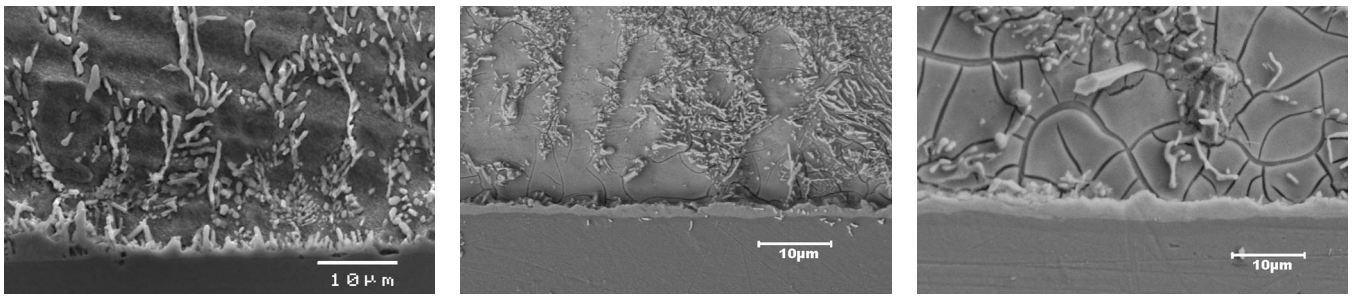

a b c

Fig. 11. IMC morphology change subject to thermal shock (SEM image): (a) 500 cycles, (b) 1,000 cycles, and (c) 2,000 cycles.

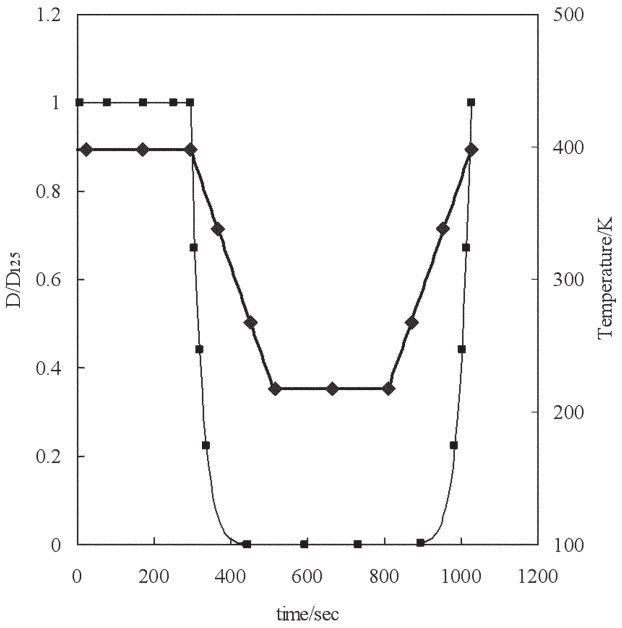

Fig. 12. Diffusion coefficient subject to time in one TS cycle: (◆) temperature and (■) diffusion coefficient.

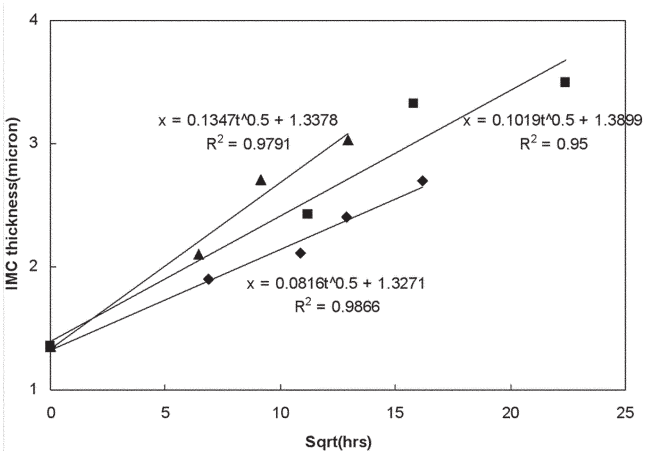

Fig. 13. Comparison of IMC data for TC, TS, and isothermal aging at 125°C: (◆)ISO 125, (■)TC, and (▲)TS.

125°C, the cycle time is 17 min and the dwell time at the upper soak temperature is 5 min. Thus, the t_{eff} for 2,000 cycles of TS aging is 10,000 min or 166.7 h.

Based on the above assumption, the IMC growth behavior measured for TC, TS, and isothermal aging at 125°C are plotted in Fig. 13. It is interesting to note that the IMC growth rates for TS and TC aging are higher than isothermal aging. And the relationship is TS > TC > isothermal. The coefficients D for TS, TC, and isothermal aging are 0.1347, 0.1019, and 0.0816, respectively. This may be due to higher thermomechanical stresses generated from nonisothermal TC and TS aging conditions. Vianco et al.[9] have noted that TC and TC can accelerate the IMC growth process compared to isothermal aging. In our study, the effect of TS aging on IMC growth rate is greater than TC aging. This suggests that stress relaxation behavior in the solder joint is not as pronounced in TS aging compared to TC aging. The TC aging has a much longer cycle time and soak period and allows further stress relaxation due to creep effects. For isothermal aging at 125°C, extensive stress relaxation in the solder is expected, and hence, the lower IMC growth rate is not accelerated by stress effects.

To quantitatively represent the acceleration effect of TC and TS aging, another parameter, "equivalent

Table I. Equivalent Isothermal Aging Time Considering the IMC Growth for TC and TS

Process Condition	Effective Time, t_{eff} (h)	IMC Thickness, x_t (μm)	Equivalent Isothermal Time, t_{eq}(h)	Accelerated Factor, $K = t_{eq}/t_{eff}$
500 TC	125	2.42	172	1.376
1,000 TC	250	3.42	643	2.572
2,000 TC	500	3.5	694	1.388
500 TS	41.7	2.1	84	2.01
1,000 TS	83.3	2.61	238	2.85
2,000 TS	166.7	2.93	375	2.24

isothermal aging time," t_{eq}, is used. This is the time required by isothermal aging to obtain the same IMC thickness compared with TC or TS aging, e.g., after 2,000 cycles of TC aging, The IMC thickness accumulated, x_t, is 3.5 μm. To obtain such an IMC thickness by isothermal aging, an equivalent time, t_{eq}, of 694 h, is needed, which is calculated by Eq. 3.

$$t_{eq} = \frac{1}{D_{iso}^2}(x_t - x_0)^2 \quad (3)$$

By comparing the previously defined effective aging time t_{eff} and t_{eq}, it is seen that t_{eff} is shorter than t_{eq}; e.g., the t_{eff} for 2,000 cycles of TS aging is 500 h, while that for t_{eq} is 694 h. This indicates that TC aging accelerated the IMC growth rate.

In the reliability test for electronic packaging, accelerated tests such as TC and TS are commonly used. An acceleration factor is defined to relate the accelerated test (under TC and TS aging) compared to isothermal aging. The acceleration factor, K, is the ratio of TC and TS, IMC growth compared to isothermal aging IMC growth. The value of K is defined as the ratio of t_{eq} divided by t_{eff}, as expressed in Eq. 4. For TC at 2,000 cycles, the accelerated factor is 1.388.

$$K = \frac{1}{D_{iso}^2 t_{eff}}(x_t - x_0)^2 \quad (4)$$

The t_{eq} and the acceleration factor for each TC and TS aging were calculated and are shown in Table I. After 2,000 cycles of TC and TS aging, the factor K is 1.388 and 2.24, respectively. This suggests that both TC and TS aging accelerate the growth of IMC due to thermomechanical stress effects expected in nonisothermal (TC and TS) aging conditions. The acceleration factor K is useful in reliability studies to develop a framework for correlating the TC, TS, and isothermal aging IMC growth database.

CONCLUSIONS

The microstructure of the 95.5Sn-3.8Ag-0.7Cu lead-free solder joint contains a Sn-rich matrix with dispersed Ag_3Sn precipitates around the Sn-rich regions and small crystals of Cu_6Sn_5 intermetallics. Large Ag_3Sn rod structures are also found in the solder joint. After reflow, the $(Ni_{1-x}Cu_x)_3Sn_4$ IMCs on the solder/nickel interface are needlelike structures. With isothermal and thermal cycling aging exposure, the IMC needles coalesce with each other, resulting in subsequent planar growth of the IMC layer.

The IMC growth subjected to isothermal and thermal cycling exposure show that the IMC layer growth rate under TC and TS aging is accelerated. An equivalent isothermal aging time is proposed for comparison of IMC layer growth data. It was noted that the IMC layer growth under TC and TS aging gave acceleration factors of 1.39 and 2.24 based on the equivalent isothermal aging time after 2,000 cycles of TC and TS aging, respectively.

ACKNOWLEDGEMENTS

John H.L. Pang acknowledges the research funding and support by the Agency for Science and Technology, the Ministry of Education of Singapore, and the School of Mechanical and Production Engineering of Nanyang Technological University.

REFERENCES

1. M.R. Harrison, J.H. Vincent and A.A.H. Steen: *Soldering Surf. Mount Technol.* 13, 21 (2001).
2. Edwin Bradley: *IEEE Proc. 2003 Electronic Components and Technology Conf.* (Piscataway, NJ: IEEE, 2003), pp. 41–48.
3. John H.L. Pang and C.K. Stephen: *Soldering Surface Mount Technol.* 14 (2002); Special Issue on Lead-Free and Lead-Bearing Solders.
4. John H.L. Pang, B.S. Xiong, and H. Kurniawijaya: *Proc. Globaltronics Technology Conf.,* Singapore, 2002, pp. 113–118, ISBN-981-04-7144-0.
5. John H.L. Pang, B.S. Xiong, and C.C. Neo: *IEEE Proc. 2003 Electronic Components and Technology Conf.* (Piscataway, NJ: IEEE, 2003), pp. 673–679.
6. H.L.J. Pang, K.H. Tan, X.Q. Shi, and Z.P. Wang: *Mater. Sci. Eng. A* 42, 307 (2001).
7. X.Q. Shi, W. Zhou, H.L.J. Pang, and Z.P. Wang: *Trans ASME, J. Electron. Packaging* 121, 179 (1999).
8. Masazumi Amagai, Masako Watanabe, and Masaki Omiya: *Microelectron. Reliability* 42, 951 (2002).
9. Paul T. Vianco, John J. Stephens, and Jerome A. Rejent: *IEEE Trans. Compon., Packaging, Manufacturing Technol.—Part A* 20, 478 (1997).
10. L.C. Shiau, C.E. Ho, and C.R. Kao: *Soldering Surface Mount Technol.* 14, 25 (2002).
11. T.Y. Lee, W.J. Choi, K.N. Tu, and J.W. Jang: *Mater. Res.* 17, 291 (2002).
12. Sung K. Kang, Paul Lauro, and Da-Yuan Shih: *Mater. Trans.* 45, 1 (2004).
13. S.W. Chen, S.H. Wu, and S.W. Lee: *J. Electron. Mater.* 32, 1188 2003.